VASP AND PROFILIN-1 INTERACTION IN CELL MIGRATION

by

David Gau

Submitted to the Graduate Faculty of

Swanson School of Engineering in partial fulfillment

of the requirements for the degree of

Bachelor of Philosophy

University of Pittsburgh

2011

UNIVERSITY OF PITTSBURGH

SWANSON SCHOOL OF ENGINEERING

This thesis was presented

by

David Gau

It was defended on

April 15, 2011

and approved by

Catherine Baty, Research Assistant Professor, Department of Cell Biology and Physiology

Frank Gertler, Professor, Department of Biology, MIT

Sanjeev Shroff, Professor, Department of Bioengineering

Thesis Director: Partha Roy, Associate Professor, Department of Bioengineering

VASP AND PROFILIN-1 INTERACTION IN CELL MIGRATION

David Gau

University of Pittsburgh, 2011

Profilins belong to a family of G-actin binding proteins which are thought to facilitate actin polymerization at the leading edge of migrating cells via its polyproline interactions with major actin nucleating and F-actin elongating proteins. The two major goals of this study are i) to spatially resolve profilins-1's (the only ubiquitously expressed member of profilin family) interaction with Ena (enabled)/VASP (vasodilator stimulated phosphoprotein) family of F-actin elongating protein, and ii) determine whether Ena/VASP regulates cell migration through its interaction with profilin-1.. This study demonstrates the feasibility of GFP (green fluorescence protein)-based florescence resonance energy transfer (FRET) to identify profilin-1 and VASP interaction. Through acceptor photobleaching FRET (fluorescence resonance energy transfer) in MDA-MB-231 human breast cancer cells, we show that VASP and profilin-1 interaction at the membrane ruffles near the leading edge. We further show that VASP overexpression in breast cancer cells results in slower random cell motility; however VASP-induced suppression of cell motility is partly rescued when VASP:profilin-1 interaction is downregulated These data suggest VASP utilizes profilin-1 to regulate breast cancer cell migration.

Table of Contents

LIST OF FIGURES

PREFACE

I would like to first and foremost thank my parents for the opportunity to attend University of Pittsburgh where I was provided all the tools and resources to become successful. Secondly, I would like to thank Dr. Partha Roy for taking a chance and allowing me to work in his lab and mentoring me through my undergraduate thesis project. Without his guidance, this document would not exist. I would also like to thank Dr. Baty, Dr. Gertler, and Dr. Shroff for being part of my thesis committee and providing insightful comments and direction towards my research and academic career in general. I also wish to thank all the members of the Roy lab that helped me and answered hundreds of my questions. These members include: Dr. Zhijie Ding, Dr. Yongho Bae, Dr. Tuhin Das, Dr. Li Zou, William Veon, Maria Jaramillo, Marion Joy, Chang Jiang, Megan Gunsaulus, and Rohit Rao. I also want to thank the Honors College for their large financial support which with without I would not have completed my studies and NIH grant CA108607. Finally, I would like to thank my amazing girlfriend Amanda Alderfer for her continuous support while I spent countless hours working on this document and keeping my spirits high always.

ABBREVIATIONS

ABPs: Actin-binding proteins

Arp: Actin-related protein

capZ: capping protein from the Z-disc of muscle

CFP: Cyan fluorescent protein

(D)PBS: (Dulbecco's) Phosphate Buffered Saline

ECM: Extracellular matrix

Ena: Enabled

EVH1: Ena-VASP homology-1

EVH2: Ena-VASP homology-2

EVL: Ena/VASP like

F-actin: Filamentous actin

FBS: Fetal bovine serum

FLIM: Fluorescence lifetime imaging measurements

FRET: Fluorescence resonance energy transfer

G-actin: Globular actin

GAPDH: Glyceraldehyde 3-phosphate dehydrogenase

GFP: Green fluorescent protein

HMEC: Human mammary epithelial cells

HUVEC: Human vascular endothelial cells

IP: Immunoprecipitation

Lpd: Lamellipodin

MDA-231: MDA-MB-231

Mena: Mammalian enabled

Pfn1: Profilin-1

PH: Pleckstrin homology

PI3K: Phosphatidylinositol 3-kinase

PI3P: Phosphatidylinositol-3-phosphate

PI(3,4)P2: Phosphatidylinositol-3,4-bisphosphate

PI(4,5)P2: Phosphatidylinositol-4,5-bisphosphate

PIP3: Phosphatidylinositol-3,4,5-triphosphate

PLC: Phospholipase-C

PPI: Phosphoinositide

PLP: Proline-rich proteins

SDS-PAGE: Sodium dodecyl sulfate polyacrylamide gel electrophoresis

siRNA: Small interfering RNA

TBST: Tris-buffered saline Tween-20

TCL: Total cell lysate

VASP: Vasodilator-stimulated phosphoprotein

WASP: Wiskott-Aldrich syndrome protein

YFP: Yellow fluorescent protein

1.0 INTRODUCTION

1.1 CELL MIGRATION

Cell migration serves an important role in both physiological and pathological processes ranging from embryonic development, angiogenesis (formation of new blood vessels) to tumor metastasis [Clainche and Carlier, 2008]. Learning about the mechanisms of how cells migrate is crucial to understanding many life processes. Migration of cells can be summarized in four steps (schematically represented in Figure 1). Cells must first polarize via cues from external factors (such as growth factors like epidermal growth factor or platelet-derived growth factor) or the microenvironment (extracellular matrix) [Panetti et al., 2004]. Once cellular asymmetry is established, F-actin polymerization at the front of the cell will create the pushing force against the cell membrane to cause membrane protrusion leading to the formation of a flat sheet-like structure called lamellipodia [Clainche and Carlier, 2008]. Actin polymerizes on the barbed or plus end of filament and depolymerizes at the pointed or minus end. This is known as actin treadmilling; faster treadmilling leads to faster protrusion. Five basic requirements must be met in order to maximize actin-based protrusions: sufficient G-actin, new actin "nuclei" generation (the beginning of an actin filament), efficient F-actin elongation, prevention of undesired growth of filaments, and nucleotide (ADP-to-ATP) exchange on actin monomers.

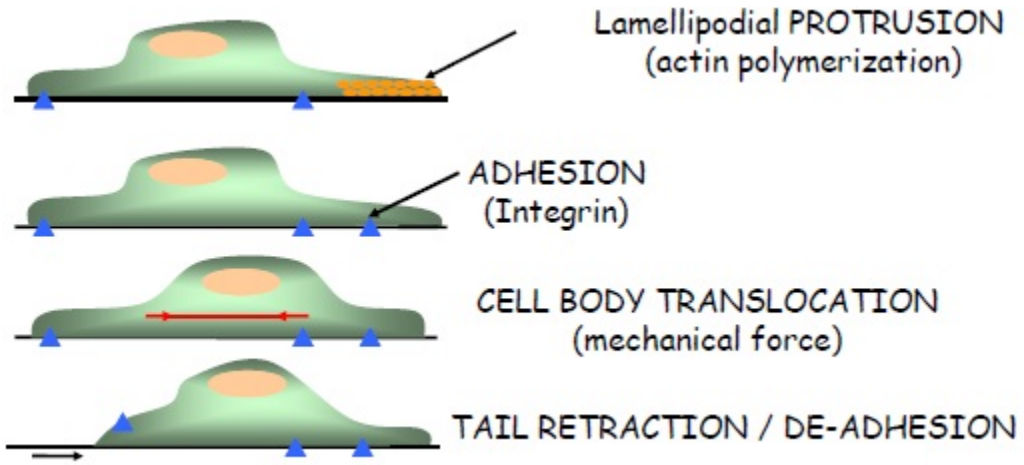

Figure 1. Four step schematic diagram of cell migration: protrusion, adhesion, contraction, and de-adhesion.

The first requirement for effective actin-based motility is having enough G-actin. This means having enough G-actin around to add to filaments. Thymosin β4 is a G-actin sequestering protein which holds G-actin and prevents it from polymerizing or nucleating, thus some actin is always available. Actin nucleation (the process describing the formation of stable actin oligomers that is capable of supporting further elongation) is catalyzed by Arp2/3 (actin-related protein) complex following its activation by WASP (Wiskott-Aldrich Syndrome Protein) family proteins [Tomasevic et al., 2007; Stradal and Scita, 2006]. Elongation of actin filaments is driven by formin (also a potent actin nucleator) and Ena/VASP family proteins. Since excessively long actin filaments tend to buckle and result in unproductive protrusions, F-actin elongation can be limited by the action of barbed-end capping proteins (example: CapZ) [note that capping also funnels actin monomers to those actin filaments which produce productive forces or allows for actin monomer use in Arp 2/3 nucleation]. Finally, actin must be regenerated in order for more polymerization to occur. Cofilin is an F-actin depolymerizing protein that binds with high affinity to ADP-actin (on the minus end) and induces a higher rate of actin depolymerization. Membrane altering enzymes such as phospholipase C-γ (PLCγ) and phosphatidylinositol 3-

kinase (PI3K) are activated downstream of receptor tyrosine kinases (RTKs) leading to the release of phospholipid-bound ABPs such as cofilin [Pollard et al., 2003; Rheenen et al., 2007]. Once ADP-actin has been detached, profilin-1 (Pfn1) works to facilitate ADP to ATP exchange on G-actin and also shuttles ATP-actin to the growing ends of F-actin. Once again, these five basic rules maximize actin treadmilling which in turn induces faster protrusion or overall net migration of cells. A summary of actin filament/nucleation elongation is shown in Figure 2.

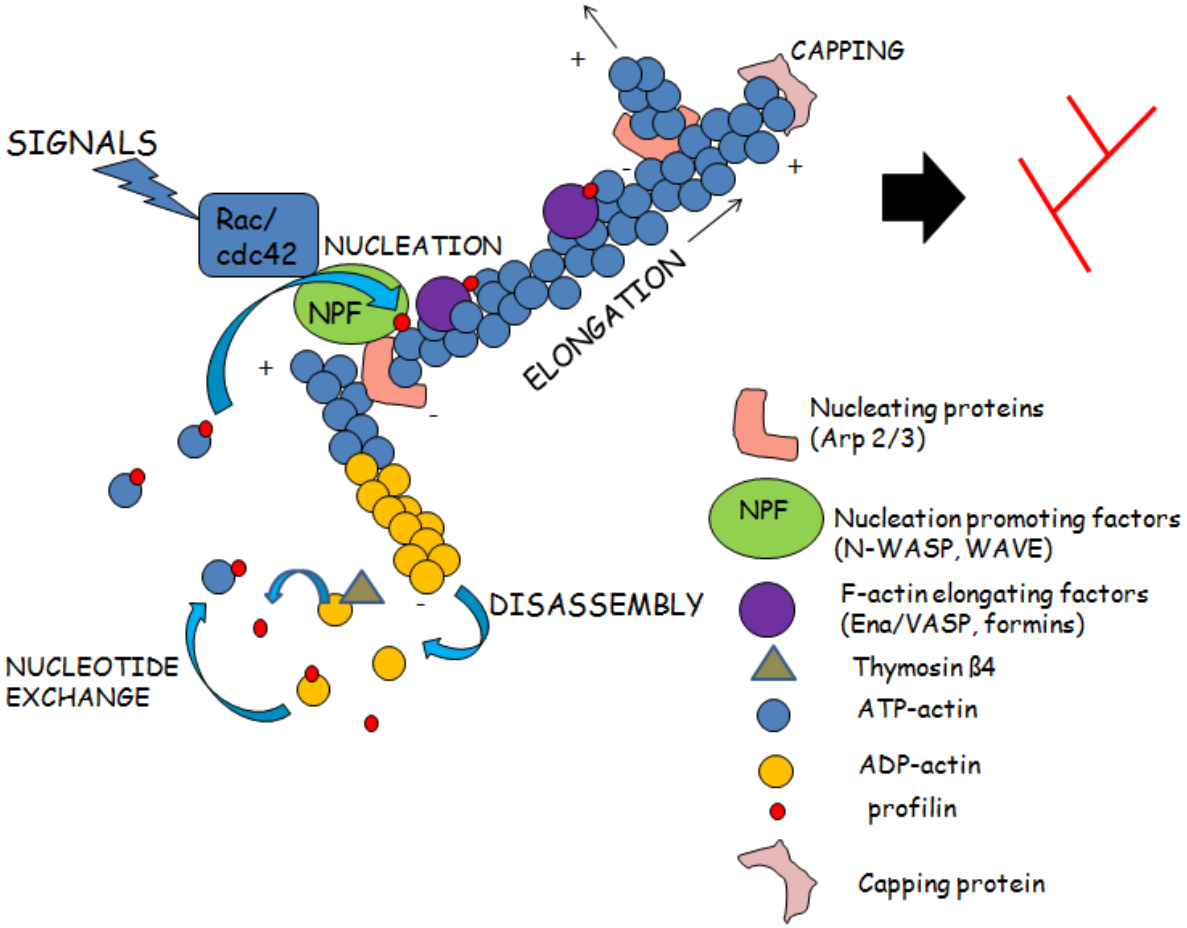

Figure 2. Actin nucleation/elongation model of actin assembly. Starting with an actin filament, first a signal will activate Rac/cdc42 which initiates a nucleation promoting factor (such as N-WASP). N-WASP then activates Arp2/3 which nucleates actin and begins a new branch on the existing F-actin. Elongating factors such as Ena/VASP or formins begin elongating new F-actin branch. Capping protein caps the growing filament which then leads to nucleation of the filament again and creates a network of branching filaments. To keep a high level of G-actin available, ADP-actin is disassembled either by itself or through cofilin. Profilin then changes ADP-actin to ATP-actin and shuttles ATP-actin to the plus ends actin filaments.

Once the cells have protruded, new attachments have to be made to ECM (extracellular matrix), i.e. basal lamina, connective tissue, through intergrins (integrins are connected to actin filaments inside cells by intracellular proteins such as talin or vinculin). Integrins can also bind to other cytosolic structures such as focal adhesion kinases (FAK) and Src family kinases to mediate actin adhesion dynamics. Creation of new adhesions works to secure protrusions in order to create a net movement [Ridley et al., 2003; Sheetz et al., 1999]. Without creation of new focal adhesions, protrusions will retract and no net movement will occur.

While the leading edge is still attached, there must be contraction followed by de-attachment of focal adhesions at the rear end. Myosin II (actin based protein in non-muscle eukaryotic cells) provides the contractile force which allows the rear of the cell to move towards the front [Sheetz et al., 1999]. Repeating these steps in a directional manner over a period of time will lead to net migration.

Since membrane protrusion is the defining step of cell migration, much work has focused on understanding the molecular controls of actin polymerization. Actin polymerization at the leading edge has been studied extensively by biomimetic assays examining F-actin driven bacterial pathogen movement (*Listeria* or *Shigella*) in either intact host cells or cellular extracts or reconstituted system consisting of purified proteins. It was shown that cofilin, capping protein, and Arp2/3 are absolutely essential for actin-based *Listeria* movement. Ena/VASP and Pfn1, although not essential, profoundly enhance the velocity of *Listeria* pathogen [Loisel et al., 1999; Geese et al., 2002]. Repeats of these experiments using N-WASP coated beads also show the same outcome [Weisner et al., 2003]. N-WASP mediated S*higella* movement, on the other hand, has been shown to absolutely require Pfn1 [Mimuro et al., 2000].

Proteins of the N-WASP, Ena/VASP, or formin family all share a common feature: the ability to bind to Pfn1 via proline-rich domains [Witke, 2004]. Nucleation and polymerization from activation of WASP, VASP and formin protein families require Pfn1 and Pfn1's ability to interact with G-actin in order to maintain full function.

1.2 PROFILIN-1

There are four types of profilin found in the mammalian genome, profilin1-4. Pfn1 (a ubiquitously expressed member of profilin and the main focus of this thesis) is found in all cell types except skeletal muscle tissue; Pfn2, which is mainly expressed in the cells of neural tissues; Pfn3 (found only in kidney and testis) and Pfn4 (only in testis) [Jockusch, 2007]. Pfn1 was initially discovered as a G-actin sequestering protein similar to thymosin β4 [Carlsson et al., 1977]; however, cellular concentration of Pfn1 was found to be insufficient to account for G-actin concentration in cells. Although binding to Pfn1 inhibits G-actin incorporation at the pointed end of actin filaments, Pfn1 is able to shuttle G-actin to the barbed ends of actin filaments. Pfn1 also facilitates the nucleotide exchange on actin (from ADP to ATP) and finally, Pfn1 displays affinity for polyproline (PLP) ligands including all major actin-nucleators (WASP, WAVE, formins) and elongating proteins (Ena/VASP, formin). These properties enable Pfn1 to facilitate actin polymerization rather than inhibit actin polymerization, as initially thought at the time of its discovery [Carlsson et al., 1977; Goldschmidt-Clermont et al., 1990; Pantaloni et al., 1993; Schluter et al., 1997; Kang et al., 1999; Bubb et al., 2003; Witke et al., 2004]. Reducing levels of Pfn1 expression led to decreased level of F-actin in various cells which further

solidifies Pfn1's role as a promoter of actin polymerization [Ding et al., 2006; Zou et al., 2007; Ding et al., 2009].

In addition to binding to actin and polyproline ligands, Pfn1 also binds to the plasma membrane by interactions with phosphoinositides (PPIs) such as phosphatidylinositol-4,5-bisphosphate (PI(4,5)P2), phosphatidylinositol-3,4-bisphosphate (PI(3,4)P2; formed from dephosphorylation of PIP3 by PI-5-phosphatase) and phosphatidylinositol-3,4,5-triphosphate (PIP3; formed from the phosphorylation of PI(4,5)P2 by PI3K). Phosphoinositide 3-kinase (PI3K) activation forms PI(3,4)P2 and PIP3 [Lu et al., 1996]. With two PPI binding regions (for mammalian Pfn1), one overlapping the actin-binding domain and the other slightly overlapping the PLP binding domain, Pfn1-PPI binding has been theorized to prevent interaction with actin [Lassing et al., 1985; Skare et al., 2002].

1.3 PROFILIN-1 AND CELL MIGRATION

A study on *Dictyostelium* ameba lacking Pfn1 and Pfn2 showed a severe defect in cell migration [Haugwitz et al., 1994]. *Drosophila* with Pfn1 mutations also exhibited defects in development [Verheyen and Cooley, 1994]. Furthermore, *C. elegans* require Pfn1 for embryogenesis [Velarde, 2007]. Silencing Pfn1 expression dramatically suppresses vascular endothelial cell motility [Ding et al., 2006; Ding et al., 2009]. Together these studies demonstrate Pfn1's role in cell migration. Pfn1's involvement in *Listeria* movement, preferential localization of Pfn1 at the leading edge and defects in protrusion resulting from Pfn1 depletion in vascular endothelial cells suggest that one of the main functions of Pfn1 is to regulate actin polymerization at the leading edge and thereby facilitate membrane protrusion and overall cell

migration [Buss et al., 1992; Mayboroda et al., 1997; Neely and Macaluso, 1997; Suetsugu et al., 1998; Mimuro et al., 2000]. Mutagenesis-based studies have shown that Pfn1's interaction with both actin and PLP ligands is important for membrane protrusion and overall migration of vascular endothelial cells [Ding et al., 2006; Ding et al., 2009]. This is consistent with a previously proposed hypothesis that PLP ligands may act to spatially regulate the location of Pfn1-actin complexes to the leading edge where actin polymerization takes place during cell migration [Holt et al., 2001].

In stark contrast to these findings, breast cancer cells and normal human mammary epithelial cells display faster migration when Pfn1 expression is silenced and overexpression of Pfn1 suppresses breast cancer cell motility [Zou et al., 2007; Bae et al., 2009]. Many invasive adenocarcinomas have low levels of Pfn1 when compared to their non-tumorigenic counterparts [Janke et al., 2000; Belot et al., 2002; Wittenmayer et al., 2004; Gronborg et al., 2006]. These data might suggest that Pfn1 has a context-specific role in cell migration. Recently, our group has shown that Pfn1 inhibits breast cancer cell motility through its membrane phosphoinositide interaction and this is independent of its actin-related activity [Bae et al., 2009].

1.4 ENA/VASP

Ena/VASP family proteins consist of three members, *Drosophila* Enabled (Ena, or Mammalian Enabled, Mena, in mammals), VASP (the focus Ena/VASP protein for the thesis), and Ena-VASP-like (EVL), all of which have been identified as regulators of actin polymerization and cell migration [Krause et al., 2003]. Conserved in the Ena/VASP family are the EVH1 (Ena/VASP homology 1) domain, proline-rich domain, and EVH2 (Ena/VASP

homology 2) domain, all of which are schematically represented in Figure 3. EVH1 domain binds to consensus site FPPPP found in focal adhesion proteins such as Zyxin, phagocytic cups of macrophages, and to *Listeria* through ActA [Krause et al., 2003]. Through this domain, Ena/VASP is recruited to focal adhesions and to the membrane as well.

The EVH2 domain contains a G-actin binding site, F-actin binding site, and a coiled-coil motif which allows for tetramerization of Ena/VASP proteins [Gertler et al., 1996; Bachmann et al., 1999]. The tetramerization of Ena/VASP family proteins via the coiled-coil domain has been shown *in vitro* to enhance actin binding and bundling [Bachmann et al., 1999; Walders-Harbeck et al., 2002]. EVH2 allows VASP to act as the actin elongator by allowing it to bind to F-actin and bring G-actin to the growing barbed end. This elongation at the barbed end has also led VASP to be considered as an anti-capper as it competes with capping proteins at the barbed ends of F-actin [Bear et al., 2002].

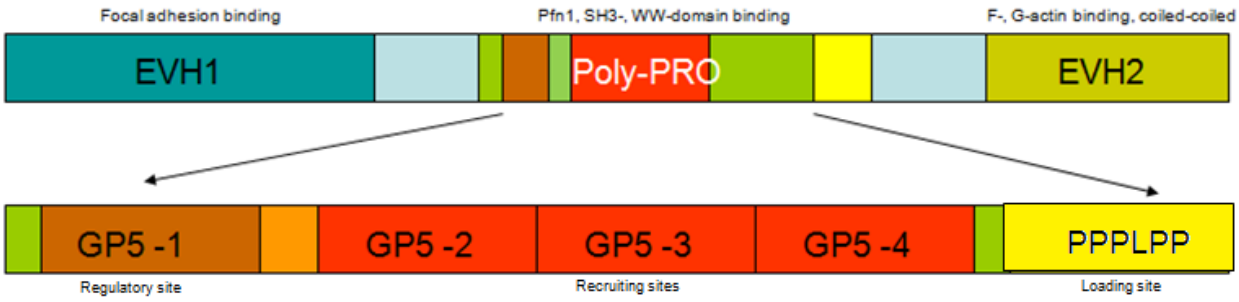

Figure 3. Conserved domains of Ena/VASP

Finally, the proline-rich domain of Ena/VASP contains sites for SH3 (Abl, Src, etc.) and WW (Utrophin, etc.) binding and for the protein Pfn1 [Krause et al., 2003]. This domain contains 3 distinct regions, a regulatory GPPPPP (GP5) site, three recruiting GP5 sites, and a loading site (schematically represented in Figure 3). The regulatory and recruiting sites recruit Pfn1 to the

proline domain with low affinity while the loading site recruits Pfn1 with 10-fold higher affinity [Ferron et al., 2007]. Recruitment of Pfn1 to the proline domain allows Ena/VASP to function at maximum capacity, at least in terms of its actin polymerizing ability and anti-capping function [Barzik et al., 2005; Hansen et al., 2010].

Like Pfn1, Ena/VASP has a context specific effect in cell migration. While speed of rapidly migrating fish keratocytes is correlated with leading edge localization of Ena/VASP proteins [Lacayo et al., 2007], fibroblast motility show the exactly opposite phenotype [Bear et al., 2000]. However, in both cell types, Ena/VASP acts as a positive regulator of membrane protrusion. This is consistent with Ena/VASP's positive effect on *Listeria* speed. Motility analyses of Ena/VASP null cells following rescue with wild-type or various deletion mutants of Ena/VASP revealed that EVH2 domain is critical but the polyproline domain of Ena/VASP is dispensable for, at least, whole cell migration. However, Ena/VASP-promoted *Listeria* motility is significantly diminished when its entire polyproline domain is deleted. Note that when GP5 sites alone were deleted leaving the loading polyproline site intact, the effect on *Listeria* motility was modest thus suggesting loading polyproline site interaction may be the predominant site [Geese et al., 2002]. Since Pfn1 binds to loading polyproline site with high affinity, it could be speculated that Ena/VASP regulates *Listeria* motility through its interaction with Pfn1 – however, this has not been directly demonstrated.

Given that *Listeria* motility has been conceived as a molecular mimicry of actin-based membrane protrusion in migrating cells, why polyproline domain deletion of Ena/VASP alters *Listeria* speed but has no effect on overall cell migration is not clear. Also since polyproline domain of Ena/VASP can bind SH3 and WW-domain proteins besides Pfn1, the role of

Ena/VASP's interaction specifically with Pfn1 in cell migration still remains unsettled in experiments utilizing deletion of polyproline domain. This will be the focus of this thesis.

2.0 HYPOTHESIS AND SPECIFIC AIMS

Ena/VASP plays a critical role in controlling actin filament geometry, membrane protrusion and the overall regulation of cell motility [Pollard et al., 2003]. Although biochemical studies have shown that Pfn1 enhances actin polymerizing and anti capping ability of Ena/VASP *in vitro* [Barzik et al., 2005; Hansen et al., 2010], the *in vivo* significance of Pfn1's interaction with Ena/VASP is somewhat unclear. While a functional polyproline domain of Ena/VASP was shown to be required for *Listeria* motility (a biomimetic readout of actin polymerization at the leading edge of migrating cells), it was dispensable for whole cell migration, at least in the case of fibroblasts. Conclusions of these studies were based on the effect of deleting the polyproline domain of Ena/VASP which not only abrogates its binding to Pfn1, but may potentially affect Ena/VASP's interaction with SH3- and WW-domain containing proteins. Therefore, there is a need to revisit these studies specifically investigating the contribution of Pfn1's interaction in Ena/VASP-mediated regulation of cell migration. Another limitation in the field is that Ena/VASP's interaction with Pfn1 has been studied almost exclusively using biochemical approaches; therefore spatiotemporal aspects of this interaction during cell migration remains unknown. I hypothesize that "**Ena/VASP regulates cell migration through its interaction with Pfn1 and Ena/VASP:Pfn1 interaction has a spatial bias in migrating cells**". To test this hypothesis, I will:

Specific Aim 1: ***Determine the spatial location of Ena/VASP:Pfn1 interaction by FRET in migrating cells (MDA-MB-231).***

Specific Aim 2: ***Determine whether Ena/VASP's effect on cell motility is influenced by its interaction with Pfn1.***

3.0 MATERIALS AND METHODS

3.1 PLASMID CONSTRUCTION AND SIRNAS

GFP-Pfn1 generation has been previously described [Roy et al., 2004]. To generate YFP-Pfn1, Pfn1 was excised from EGFP-Pfn1 vector and subcloned into EYFP-C1 vector at Hind3 and BamH1 restriction. YFP-Pfn1 was also subcloned into ECFPN1 vector at EcorR1 and Kpn1 restriction sites to generate the chimeric YFP–Pfn1–CFP (YPC) construct. Myc-tagged YFP-Pfn1 construct (myc-YFP-Pfn1) was generated by subcloning YFP-Pfn1 into a pCMV-myc expression vector at EcoR1 and Kpn1 restriction sites. Full-length VASP cDNA (PCR amplified from a human cDNA library) was subcloned into ECFP-C1 vector at Hind3 and BamH1 restriction sites. Pfn1-shRNA was constructed by ligating a commercially available vector pRFP-C-RS (Origene Technologies Inc., Rockville, MD) with a custom-designed 21-mer hairpin sequence targeting Pfn1 at BamH1 and Hind3 sites. The sense sequence for the Pfn1-shRNA is 5'-GAT CGA AGA AGG TGT CCA CGG TGG TTA AGT TCT CTA ACC ACC GTG GAC ACC TTC TTT TTT TTG GAA A-3'; the antisense sequence is 5'-AGC TTT TCC AAA AAA AAG AAG GTG TCC ACG GTG GTT AGA GAA CTT AAC CAC CGT GGA CAC CTT CTT C 3'. A control shRNA vector against luciferase (luc-shRNA) was also constructed in the same manner with the sense sequence: 5'-GAT CGG CTT ACG CTG AGT ACT TCG ATT CAA GAG ATC GAA GTA CTC AGC GTA AGC TTT TTT GGA AA-3', and the antisense

sequence: 5'-AGC TTT TCC AAA AAA GCT TAC GCT GAG TAC TTC GAT CTC TTG AAT CGA AGT ACT CAG CGT AAG CC-3'. H133S mutation in Pfn1-coding region of YFP-Pfn1 and myc-YFP-Pfn1 was executed by site-directed mutagenesis as previously described [Zou et al., 2007]. All Pfn1 constructs were made Pfn1-siRNA-resistant by placing a silent mutation in the siRNA targeting region without changing the peptide encoding (targeting region of Pfn1-siRNA has been previously described [Ding et al., 2009]). VASP siRNA targeted to the untranslated region (GAGUGAAUCUGCGCGGAGA), UTR, and Mena siRNA targeted to the open reading frame (GAGAGAGAGCGCAGAAUAU), ORF, were purchased from Dharmacon (Lafayette, CO). Mutagenesis of enhanced green fluorescent protein (EGFP)-tagged full length VASP regulatory GP5 site P120 and loading site L210 was done using PCR-based site-directed mutagenesis. The forward and reverse primers for P120E mutant were 5' - GGA GGT GGG CCC CCT GAA CCC CCA GCA CTT CCC - 3' and 5' – GGG AAG TGC TGG GGG TTC AGG GGG CCC ACC TCC - 3' respectively. The forward and reverse primers for L210E mutant were 5' – CCC CCT GCA CCC CCT GAA CCG GCA GCA CAG GGC - 3' and 5' – GCC CTG TGC TGC CGG TTC AGG GGG TGC AGG GGG - 3' respectively. EGFP-VASP with regulatory and loading site mutations was made as follows. EGFP-VASP was first mutated at P120 and then that modified vector was mutated at L210. All constructs were confirmed by DNA sequencing.

3.2 CELL CULTURE AND TRANSFECTION

HEK293 cells were cultured in DMEM-F12 media supplemented with 10% fetal bovine serum (FBS) and antibiotics (Invitrogen - Carlsbad, CA). MDA-231 breast cancer cells were

cultured in EMEM media and supplemented with 10% FBS, sodium pyruvate and antibiotics. MDA-231 stably transfected with Pfn1- and Luc shRNA were selected and maintained as stated above with additional 250 ng/mL puromycin. MDA-231 cells stably transfected with EGFP or EGFP VASP constructs using Lipofectamine 2000 reagent (Invitrogen- Carlsbad, CA) were maintained in media as above and supplemented with 500 μg/ml G418. The working concentration for various siRNAs were: Pfn1 (50 nM for MDA-231) , VASP (100 nM), and Mena (100 nM). SiRNA transfection was performed using reagents commercially available from Dharmacon (Lafayette, CO) following the manufacturer's protocol. All silencing-based experiments were performed 72 hours after transfection.

3.3 ANTIBODIES

Monoclonal GFP (1:1000), VASP (1:1000) and vimentin (1:1000) antibodies were obtained from Pharmingen (San Diego, CA). Polyclonal GFP antibody was obtained from Abcam (Cambridge, MA). Polyclonal VASP antibody was obtained as a generous gift from Dr. Frank Gertler (MIT; Cambridge, MA). Polyclonal Pfn1 (1:1000) and monoclonal Mena (1:200) antibodies were obtained from Santa Cruz Biotechnology (Santa Cruz, CA). Monoclonal GAPDH (1:2000) antibody was obtained from Abd Serotec (Raleigh, NC). Polyclonal myc (1:2000) antibody was obtained from Sigma Aldrich (St. Louis, MO).

3.4 PROTEIN EXTRACTION / IMMUNOBLOTTING

Total cell lysate (TCL) was prepared by first washing cells with cold DPBS and then extracting cells with modified RIPA buffer (50 mM Tris-HCL—pH 7.5, 150 mM NaCl, 1% triton-X100, .25% sodium deoxycholate, 0.1% SDS, 2 mM EDTA, 50 mM NaF, 1 mM sodium pervanadate, 10 μg/mL leupeptin, aprotinin, pepstatin and 1 mM phenylmethylsulfonyl fluoride. The lysates were clarified at 13,000 rpm for 10 min at 4 ^{o}C and the protein concentration was determined using a coomassie-based protein assay kit (Pierce; Rockford, IL). For protein electrophoresis, equal amounts of protein samples were loaded on a SDS-PAGE and transferred onto a nitrocellulose membrane. After blocking the membrane with 5% non-fat dry milk in TBST for 1 hour at room temperature, immunoblotting was performed overnight with the appropriate antibodies. After extensive washing with TBST, the blot was incubated with the appropriate secondary antibody (1:1000 dilution, Pharmingen, San Diego, CA) and washed 3 times with TBST before performing chemiluminescence for the visualization of protein bands.

3.5 FLUORESCENCE RESONANCE ENERGY TRANSFER (FRET)

For spectral FRET analyses, cells expressing FRET constructs (YFP-Pfn1:CFP-VASP, YFP-Pfn1 H133S:CFP-VASP, YPC) were trypsinized and resuspended in PBS before an emission scan was performed on cell suspension for a wavelength range of 465–600 nm corresponding to 425 nm excitation using a spectrofluorophotometer (spectral scan was gathered within 10 min of trypsinization). For imaging experiments, cells expressing various FRET constructs were allowed to form a monolayer on collagen coated glass cover slips and then

scratched using a pipet-tip. Cells migrated for 6–8 h before fixing them with 4% formaldehyde for 15 minutes, washed with DPBS after, and then mounted on slides. Acceptor photobleaching was then performed on cells that display polarized morphology (these cells are typically located on the edge of the wound and tend to be most motile before fixation) on a Zeiss LSM 510 Meta confocal microscope (Carl Zeiss. Inc., Thornwood, NY) coupled to an argon laser. Cells were bleached at the region of interest (ROI) with 514 nm wavelength on 50% laser power, and the bleaching duration ranged from 10 to 20 s (for ROI bleaching) to ~1 min (for whole cell bleaching). Cells were imaged with a 63x 1.4 NA Zeiss oil immersion objective at either 2x or 4x zoom. CFP and YFP images were acquired with laser power set at 33% (458 nm) and 7.5% (488 nm), respectively. To calculate FRET efficiency, multiple 120-pixel long lines within ROI were constructed from the edge of the cell into the cytoplasm; the average intensity of these line scans in CFP channel before bleaching was subtracted from the corresponding value recorded after bleaching and then normalized to the pre-bleaching value.

3.6 SINGLE-CELL MIGRATION ASSAY

MDA-231 with different treatments, were sparsely plated (1.5-3.5 x 10^4 cells) on a 35 mm plastic tissue-culture dish coated with collagen. After incubation overnight, time-lapse videomicroscopy of 9 random phase contrast fields with 10x objective were simultaneously performed at an interval of 1 minute for a total duration of 120 minutes. For all time-lapse imaging, optimal environmental conditions, 37°C and pH 7.4, were maintained by a microincubator. Cell trajectory was built via frame-by-frame analyses of the centroid positions (x, y) of cell-nuclei (which were assumed to be the fair representation of the cell body).

Protrusion direction was determined by creating a vector from the centroid of a cell-nuclei and the furthest point of a protrusion before protrusion is retracted. Persistence was calculated using a non-overlapping interval random walk model as previously described [Dickenson and Tranquillo, 2004] The acquired images were analyzed using the NIH ImageJ software.

3.7 STATISTICS AND DATA REPRESENTATION

All statistical tests were performed with ANOVA followed by Tukey-Kramer post-hoc test analysis. P values less than 0.05 were considered to be statistically significant. In most cases, experimental data was represented as box and whisker plots where crosses represents the mean, middle lines of box indicates median, top of the box indicates 75th percentile, bottom of the box measures 25th percentile and the two whiskers indicate the 10th and 90th percentiles, respectively.

4.0 SPATIAL INTERACTION OF PFN1 AND VASP

From previous experiments, we have learned that Pfn1 is important in motility. For example, there is evidence of motility defect when Pfn1 and 2 are suppressed in *Dictyostelium* amebae [Haugwitz et al., 1994]. In addition, *Drosophila* expressing a mutant Pfn1 [Verheyen et al., 1994] and Pfn1 deficient human vascular endothelial cells [Ding et al., 2006] show defects in cell migration. These effects, however, depend on the cell type as silencing Pfn1 in invasive breast cancer cells increase cell motility while overexpression leads to a reduction in cell motility [Roy et al., 2004; Zou et al., 2007; Bae et al., 2009]. Pfn1 interaction with PLPs has also been shown to be important for cell migration [Ding et al., 2006; Ding et al., 2009] but specific interaction has never been shown.

Specific Aim 1: ***To determine spatially where Pfn1 and VASP interact in motile cells (human breast cancer cells)***

This chapter has been published in the following:

Gau, D, Ding Z, Baty C, Roy P. (2011) Fluorescence Resonance Energy Transfer (FRET)-based detection of profilin-VASP interaction. *Cell. Mol. Bioeng.* **4**, 1-8.

4.1 RESULTS

4.1.1 Generation of FRET constructs

Pfn1 interaction with Ena/VASP has been investigated in the past using biochemical techniques; however biochemical techniques [Reinhard et al., 1995] do not allow for spatial recognition of where the protein-protein interaction takes place. To show where Pfn1:VASP interaction take place, we utilized a technique called fluorescence resonance energy transfer (FRET). FRET utilizes energy transfer from one excited fluorescent molecule (designated as the donor) to another close and unexcited fluorescent molecule (designated as the acceptor) such that the acceptor will emit a fluorescent signal and the emission signal of the donor decreases. When two proteins that are potentially interacting with each other are conjugated with donor and acceptor fluorophores, the association may be visualized by FRET [Roy et al., 2002]. Note that the work done in the next three figures was performed by Dr. Partha Roy.

First and foremost, CFP and YFP FRET pair constructs were generated and schematically represented in Figure 4a (CFP is fused to VASP while YFP is fused to Pfn1). CFP and YFP (CFP and YFP are a suitable FRET pair as CFP excitation level is distinct from YFP excitation however CFP emission will excite YFP) conjugated to VASP and Pfn1 respectively were created via N-terminus fusion. Fusion of GFP to the N-terminus typically roughly creates a 50% reduction in polyproline binding but no side effects to actin or phospholipid binding of Pfn1 [Gau et al., 2011]. Despite the reduction of polyproline binding due to GFP conjugation, this is an acceptable strategy as fusion of GFP to the C-terminus abolishes Pfn1's ability to bind polyproline. In addition, GFP-Pfn1 has been shown to still localize in similar regions as endogenous Pfn1 while Pfn1-GFP does not [Wittenmayer et al., 2000]. It has also been

previously shown that GFP binding to the N-terminus of VASP has been used as a live-cell reporter for VASP [Rottner et al., 1999]. Additionally, an H133S point mutation form of Pfn1 was generated on YFP-Pfn1 as a negative control. This mutant should have very little to no binding ability to any PLPs including VASP [Zou et al., 2007]. In addition to the CFP and YFP tag, myc-tag was introduced to the YFP constructs which enables specific immunoprecipitation of YFP-Pfn1 and YFP-Pfn1 H133S. Myc-tag was included to all Pfn1 mutants because anti-GFP antibody recognizes both CFP and YFP, thus preventing the specificity of immunoprecipitation. Addition of myc-tag allowed for discrimination between YFP-Pfn1 and CFP-VASP. A positive control of YFP-Pfn1-CFP (YPC) was also created to force a strong intramolecular FRET signal. Figure 4b shows the constructs after transient transfection in HEK293 cells.

To confirm *in vivo* binding of CFP-VASP and myc-YFP-Pfn1, the constructs were co-expressed in HEK293 cells by transient transfection. As a negative control, either CFP-VASP was co-expressed with myc-YFP-Pfn1-H133S or CFP with myc-YFP-Pfn1. Anti-myc immunoprecipitates, when probed with GFP antibody, show that CFP-VASP co-precipitated with myc-YFP-Pfn1 as expected (Figure 5). This is due to interaction between VASP and Pfn1 since CFP-VASP failed to co-precipitate with the H133S mutant form of Pfn1 and CFP did not co-precipitate with myc-YFP-Pfn1 which rules out the possibility of CFP-YFP heterodimer formation. These immunoprecipitation results also confirm that addition of CFP or YFP tags still allows *in vivo* interaction between Pfn1 and VASP.

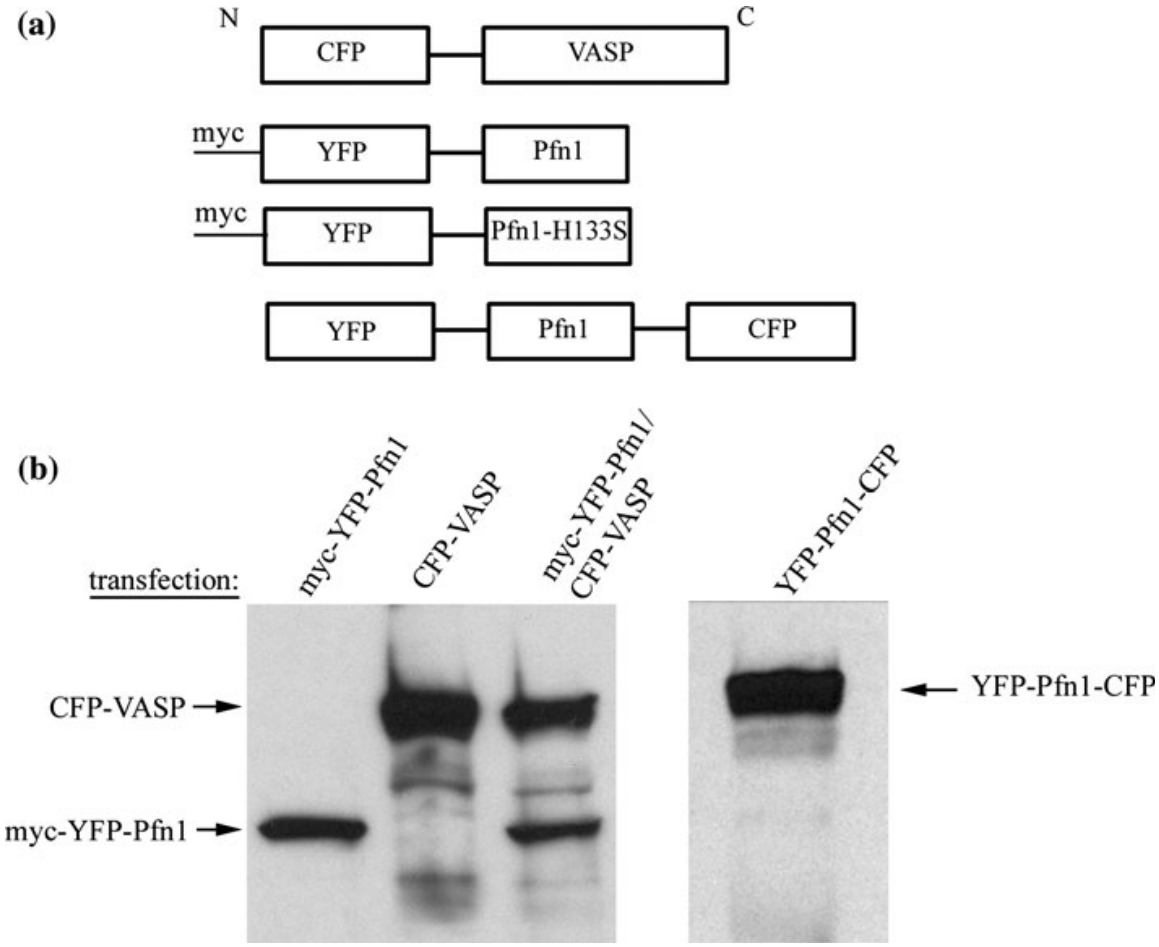

Figure 4. Creation of FRET constructs. (a) Schematic diagram of various FRET constructs. (b) GFP-immunoblot showing expression of various FRET constructs after 48 hrs transient transfection on HEK293 cells.

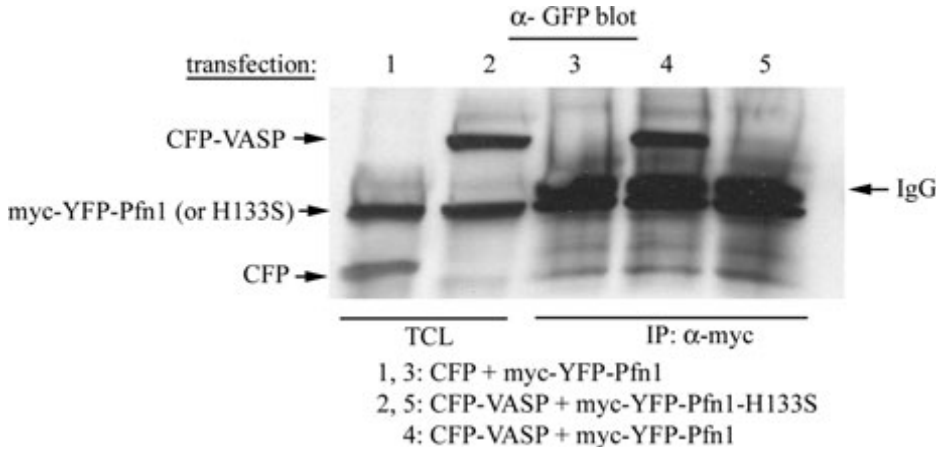

Figure 5. Co-IP of FRET constructs. Myc-YFP-Pfn1 or H133S mutant co-expressed with either CFP or CFP-VASP in HEK293 cells. When immunoprecipitated with anti-myc and probed with GFP antibody, only binding between CFP-VASP and myc-YFP-Pfn1.

4.1.2 Spectral FRET of Pfn1:VASP

Next, to see whether Pfn1:VASP interaction can be resolved using spectral FRET, the constructs were again co-expressed as before in HEK293 cells. As additional negative controls, CFP-VASP was expressed alone and CFP was co-expressed with YFP-Pfn1. As a positive control, YPC was expressed alone in HEK293 cells. Cell suspension was excited at 425 nm wavelength (maximum excitation wavelength for CFP) and resultant emission spectrum over wavelength range of 460 to 600 nm was obtained at 5 nm intervals. Figure 6a shows the emission spectra data from the different groups. Cells expression CFP-VASP only showed one peak at 470 nm as expected while cells expressing both CFP-VASP and myc-YFP-Pfn1 showed two peaks at 465 and 520 nm wavelength (this was determined to be the FRET signature as it was seen in the positive control YPC expressing group). The two peaks were not detected in cells co-expressing CFP-VASP and myc-YFP-Pfn1-H133S. Cells in a suspended nature however do not mimic natural condition for cells which are non-hematopoietic, i.e. HEK293 cells. To investigate whether adherent vs. suspended states has any influence on Pfn1:VASP interaction in cells, GFP-Pfn1 was expressed in HEK293 cells and endogenous VASP binding via immunoprecipitation of GFP-Pfn1 was examined between cells in adherent and suspended states. Figure 6b shows that VASP:Pfn1 interaction decreases greatly when cell-substrate adhesion is lost. Thus, the spectral FRET signal between CFP-VASP and YFP-Pfn1 is likely an underestimation of the actual interaction in the the adherent state..

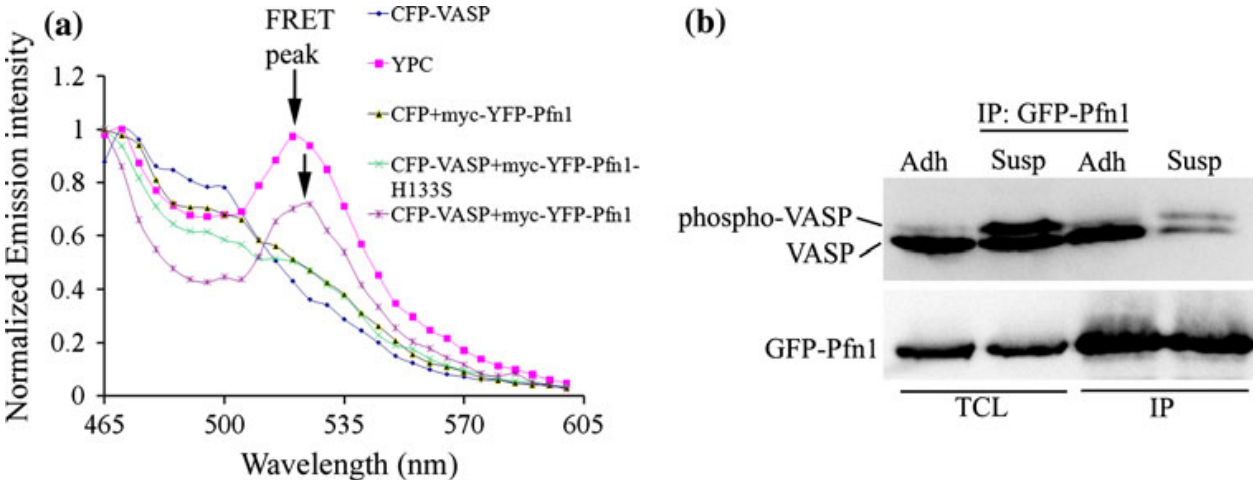

Figure 6. Spectral FRET of FRET constructs in suspension. (a) Emission spectra of cells expression various FRET constructs under 425 nm excitation wavelength. FRET peak is shown by the arrow. Cells expressing the positive control YPC or co-expressing CFP-VASP and myc-YFP-Pfn1 show evidence of spectral FRET (all intensity values are normalized with the peak value at around 465-470 nm). (b) VASP blot (top panel) shows a remarkable difference in binding of endogenous VASP to GFP-Pfn1 via IPs between suspension (susp) and adherent (adh) states of HEK293 cells. GFP blot (bottom panel) is acting as a loading control for TCL and IP samples (TCL—total cell lysate; IP—immunoprecipitation).

4.1.3 FRET between Pfn1 and VASP is detected at membrane ruffles near leading edge

In order to determine if visualization of Pfn1:VASP interaction is possible in cells, we chose MDA-MB-231 (MDA-231) breast cancer cells which are highly motile and display a polarized (defined front and rear) morphology in culture. Since endogenous Pfn1 may compete with CFP-VASP binding and lower FRET signal, experiments were conducted on MDA-231 stably expressing Pfn1-shRNA or luc-shRNA (control). Figure 7a immunoblot shows strong suppression of endogenous Pfn1 in Pfn1-shRNA expressing groups. As previously stated, all Pfn1 constructs are mutated in the silencing targeting region of siRNA or shRNA so that it will not be affected. Using acceptor photobleaching FRET (where YFP is the acceptor and CFP is the donor) we show in Figure 7b pre- and post-bleach CFP- and YFP-channel images of Pfn1-shRNA MDA-231 cells co-expressing CFP-VASP with either YFP-Pfn1 or YFP-Pfn1-H133S. The region boxed for the YFP channel shows region where YFP bleaching occurred and thus

lower YFP expression. When the CFP expression was compared between CFP-VASP/YFP-Pfn1 group and CFP-VASP/YFP-Pfn1-H133S group, we noticed that the pseudocolor plot intensity increased for YFP-Pfn1 co-expressed with CFP-VASP and not for the other. The lack of change in intensity for CFP-VASP/YFP-Pfn1-H133S was expected as the H133S mutation prevents binding of Pfn1 with PLPs, thus no FRET. Figure 8c shows the quantification of intensity change (~20% positive increase with CFP-VASP co-expressed with YFP-Pfn1 vs. -.8% for CFP-VASP co-expressed with YFP-Pfn1-H133S). A negative change in intensity is not unusual as it may occur from repetitive fluorescence imaging and thus photobleaching of flurophores [Karpova et al., 2003].

Next, to determine sub cellular localization of Pfn1:VASP interaction, acceptor photobleaching was performed on a whole cell level. Pseudocolor plots (Figure 8) of co-expressing CFP-VASP and YFP-Pfn1 in CFP channel show increase in CFP-fluorescence on membrane ruffles of protruding lamellipod (shown with arrows) and in a somewhat diffuse fashion in the perinuclear region (shown with arrowhead). YFP-fluorescence partially decreased post bleaching as desired (Figure 8 upper panel). In order to determine that successive imaging was not the cause of CFP intensity increase, CFP and YFP images were taken in a similar fashion as for photobleaching except photobleaching was not performed. As shown by the bottom panel of Figure 8, CFP intensity increase was not due to successive image acquisition.

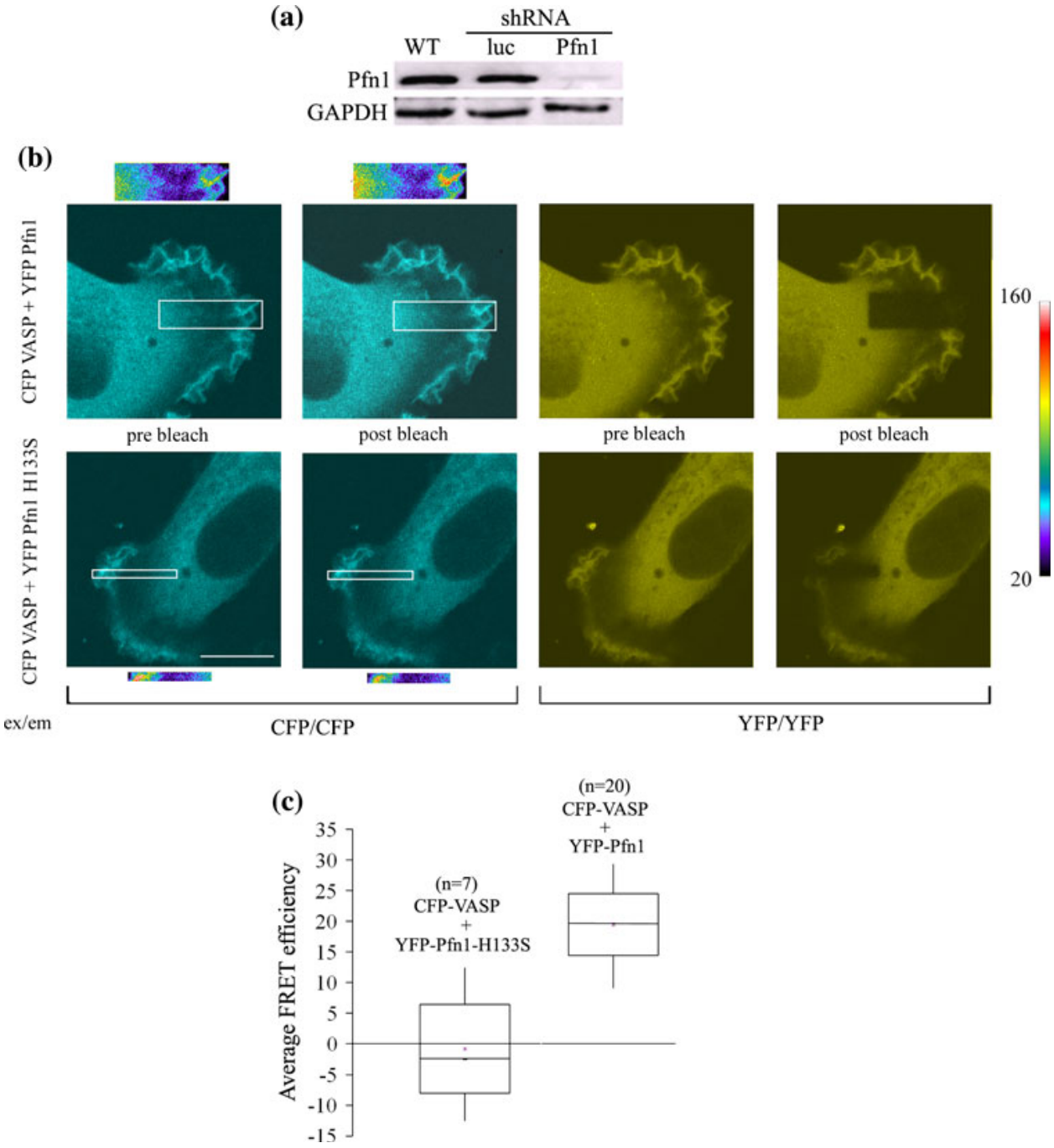

Figure 7. Visualization of Pfn1:VASP interaction using acceptor photobleaching FRET. (a) Pfn1 immunoblot of TCL extracted from wild type and various stable shRNA-expressers of MDA-231 cells depicting strong suppression of endogenous Pfn1 expression in Pfn1-shRNA expressers (luc—luciferase acts as a control for shRNA). GAPDH blot serves as the loading control. (b) Pre- and post-bleach images of MDA-231 co-expressers of either CFP-VASP/YFP-Pfn1 or CFP-VASP/YFP-Pfn1-H133S in CFP and YFP channels (boxes outline the region of bleaching and insets show pseudocolor plots of the bleached region). (c) A box and whisker plot comparing the average FRET efficiency between the two test conditions (n—number of analyzed cells pooled from 2 to 3 experiments; ex: excitation, em: emission; bar—20 µm).

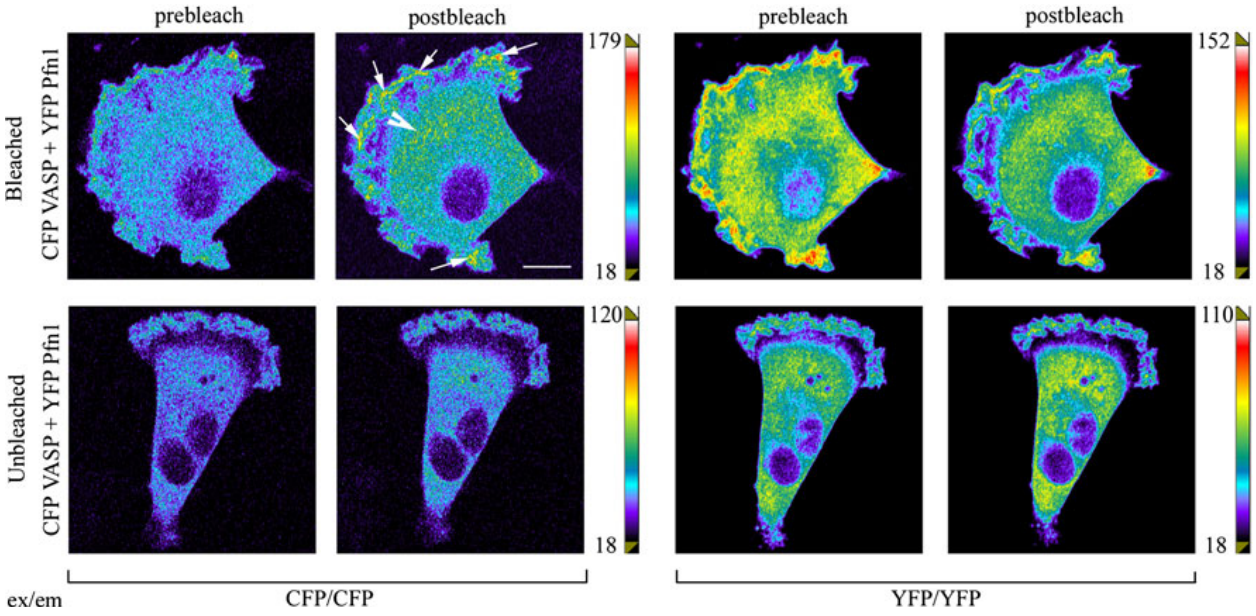

Figure 8. FRET occurs at the membrane ruffles near the leading edge. Pseudocolor plots of CFP and YFP images from cell co-expression CFP-VASP and YFP-Pfn1 pre- and post-photobleaching of the whole cell (Top panel depicts representative image of 10 cells). Arrows indicate FRET at membrane ruffles. Arrowhead shows some diffuse FRET in the perinuclear region. Bottom panel shows a cell that is not photobleached but imaged successively as before (representative image of 3 cells) (ex: excitation; em: emission; bar—20 µm).

4.2 DISCUSSION

Much work has been done thus far in the field to elucidate the role of Pfn1 in cell migration. Pfn1's role however is dynamic and depends on the system being investigated, for example in invasive breast cancer cells, silencing Pfn1 increases cell motility while overexpression leads to a reduction in cell motility while in human endothelial cells, silencing Pfn1 leads to defects in migration [Roy et al., 2004; Ding et al., 2006; Zou et al., 2007; Bae et al., 2009]. Interaction between Pfn1 and PLPs has been shown previously to be important for cell migration [Ding et al., 2006; Ding et al., 2009]. Specific interaction between Pfn1 and PLPs regarding spatial interaction has not been investigated previously however. In this study, we

show the spatial interaction between Pfn1 and one of its PLP binding partners VASP using FRET.

In terms of analyzing FRET, the most widely adopted method is measuring acceptor emission after donor excitation. This method has some drawbacks such as bleed-through of donor emission into the acceptor channel and cross-excitation of acceptor molecule by donor excitation wavelength. Mathematical correction would be required to convert raw FRET images to real FRET images. These issues become significant if the FRET signal is low because the signal can be masked by donor bleed-through and/or acceptor cross excitation, particularly with CFP- and YFP- based models due to the large spectral overlap of the two. To overcome this issue, acceptor photobleaching FRET was used. This technique relies on the fact that energy transfer between donor and acceptor is reduced when the acceptor is photobleached which causes an increase of emission for the donor. This method does not require any rigorous image correction via mathematics like conventional FRET imaging and is also better for investigating protein-protein interaction as fluorescence is generally decreased through photobleaching anyways unless there is FRET [Karpova et al., 2003]. As shown earlier, FRET was indeed detected by CFP-VASP/YFP-Pfn1 co-expressers and not by CFP-VASP/YFP-Pfn1-H133S co-expressers. One downside to acceptor photobleaching is attempting to photobleach live cells. Heavy laser exposure might kill cells while trying to photobleach the acceptor.

From the whole cell bleaching images, FRET seemed to occur at the membrane ruffles in the protruding lamellipod and somewhat in a diffuse fashion in the perinuclear region. Leading edge membrane ruffles are areas of high actin dynamics. For example, fibroblasts have shown that Ena/VASP activity leads to increased rates of membrane protrusion but these protrusions tend to be unstable and are retracted frequently [Bear et al., 2002]. Unproductive protrusions

cause membrane ruffles most of the time. Due to this, it is not unlikely that Pfn1:VASP interaction would be seen at the ruffles. Why Pfn1:VASP FRET is occurring in the perinuclear region is unclear.

To summarize, we were able to elucidate using an intermolecular FRET technique the spatial interaction of Pfn1 with one of its key PLP partner VASP. Despite the usefulness of acceptor photobleaching with spatially resolving protein-protein interaction in cells, acceptor photobleaching is not able to demonstrate dynamics of interaction. Future experiments should consider fluorescence lifetime imaging measurements (FLIM)-based FRET technique to look at spatiotemporal dynamics of Pfn1:VASP interaction during cell migration. Now that Pfn1:VASP interaction has been shown, the next question is the effects of the interaction. This will be looked into with ***Specific Aim 2***.

5.0 ROLE OF ENA/VASP:PFN1 INTERACTION IN CELL MIGRATION

Previous studies have shown that Pfn1 enhances the actin polymerizing and anti capping aspect of VASP [Barzik et al., 2005; Hansen et al., 2010]. The polyproline domain of VASP was also demonstrated to be necessary for *Listeria* motility but not as necessary for whole cell migration for at least fibroblasts. *In vivo* importance of Ena/VASP and Pfn1 interaction are not well described however. In addition, previous studies on polyproline domain of VASP involved deletion of the polyproline domain which not only abrogates binding to Pfn1, but also potentially affects interaction with SH3- and WW-domain containing proteins. Thus, the role of Pfn1's interaction in Ena/VASP-mediated regulation of cell migration must be specifically examined

Specific Aim 2: ***Determine whether Ena/VASP's effect on cell motility is influenced by its interaction with Pfn1.***

.

5.1 RESULTS

5.1.1 Mena/VASP knockdown negatively regulates cell migration

To address whether Ena/VASP proteins play a role in MDA-231 cell motility, I performed silencing experiments where VASP and Mena, two important members of Ena/VASP protein family, were transiently knocked down either selectively or in combination (as control, cells were transfected with non-targeting control siRNA). Immunoblot data in Fig 9a shows strong suppression of Mena and VASP expression in MDA-231 cells after respective siRNA treatment. I first analyzed the phenotypes of these different groups of cells by phase-contrast microscopy. Interestingly, a significant fraction (~50%,) of Mena/VASP knockdown cells displayed a highly elongated morphology lacking a robust lamellipodia (Figures 9b and 9c). This phenotype was also seen in cells subjected to either VASP or Mena knockdown, but not as pronounced as seen in cells with dual knockdown of Mena and VASP. Mena knockdown seemed to elicit a stronger phenotype than VASP knockdown in terms of suppressing lamellipodial formation in MDA-231 cells. Overall, these data are consistent with Ena/VASP's role in lamellipodial protrusion.

I next determined random motility of MDA-231 cells following Mena and VASP knockdown, the results of which are shown in Figure 9d. VASP knockdown alone had no effect on the average speed of randomly migrating MDA-231 cells. Silencing Mena alone reduced the average speed by about 15% ($p<0.05$). Even though dual suppression of Mena and VASP induced a strong morphological phenotype, surprisingly, the average speed was only moderately affected. Silencing Mena and VASP reduced the average speed by only 25% ($p<0.01$). The

impaired speed was partly due to some cells not migrating when there were many elongated lamellipodia. I did not find any statistical difference in the average speed between Mena- and Mena/VASP- knockdown groups.

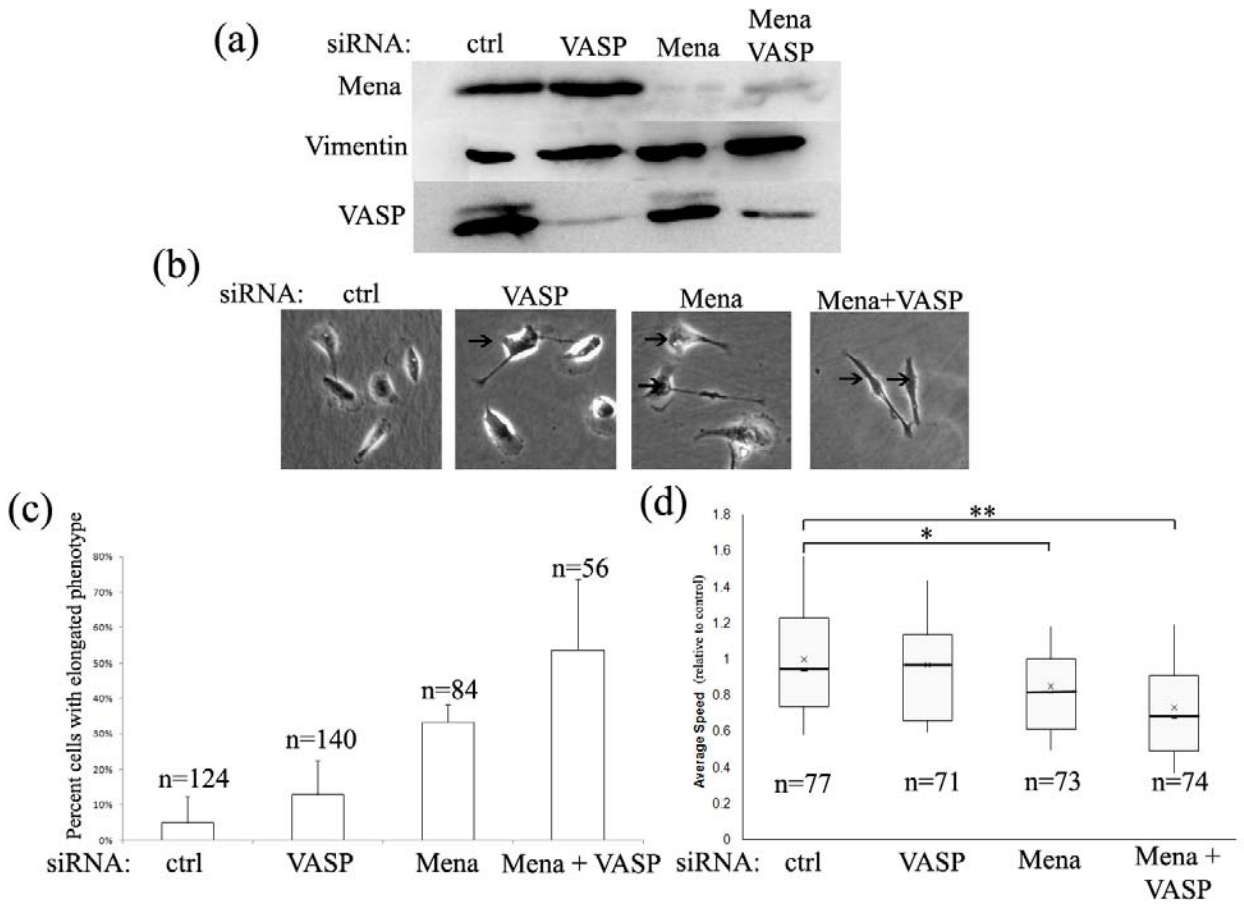

Figure 9. Mena/VASP knockdown slightly reduces motility. (a) Immunoblot of ctrl, VASP, Mena, and Mena/VASP siRNA MDA-231 cells. Vimentin is used as a loading control. (b) Representative images from four siRNA groups. Lamellipodial defect phenotype indicated by arrows. (c) Bar graph representing number of elongated lamellipodia cells (n represents total number of cells from three experiments). (d) Box and whisker plot representing average speed of ctrl, VASP, Mena, and Mena/VASP siRNA groups. Asterisk and double asterisks represent P<.05 and P<.01 respectively.

5.1.2 VASP overexpression reduces average migration speed in MDA-231

Since Mena/VASP knockdown failed to induce a dramatic change in the random motility of MDA-231 cells, I next studied the effect of VASP overexpression on MDA-231 cell motility. I created a stable subline of MDA-231 cells overexpressing GFP-VASP. Immunoblot of total lysate derived from MDA-231 sublines expressing either GFP-VASP or GFP (control) showed about 3.5 fold overexpression of VASP in GFP-VASP expressers (note that endogenous VASP expression level is unchanged). Single-cell random motility assay was then conducted to determine the effect of VASP over-expression, the results of which are shown in Figure 10. GFP-VASP overexpression caused a 2-fold reduction in the migration speed. GFP-VASP overexpressers also seemed to be 50% less persistent in their direction of motility compared to GFP expressers (Figure 11). Overall, GFP-VASP overexpressers showed a tendency to initiate more frequent protrusions in random directions than GFP expressers which could very well explain reduced persistence of motility for this cell line. Finally, to confirm that VASP overexpression induced suppression of MDA-231 motility is not due to a clonal artifact, I examined the effect of transient overexpression of GFP-VASP on the random motility of MDA-231 cells (control cells were transiently transfected with GFP-encoding plasmid). The experimental outcome (i.e., ~2-fold reduction in speed caused by VASP overexpression) (Figure 10c) was comparable to my previous finding with the stable overexpressers.

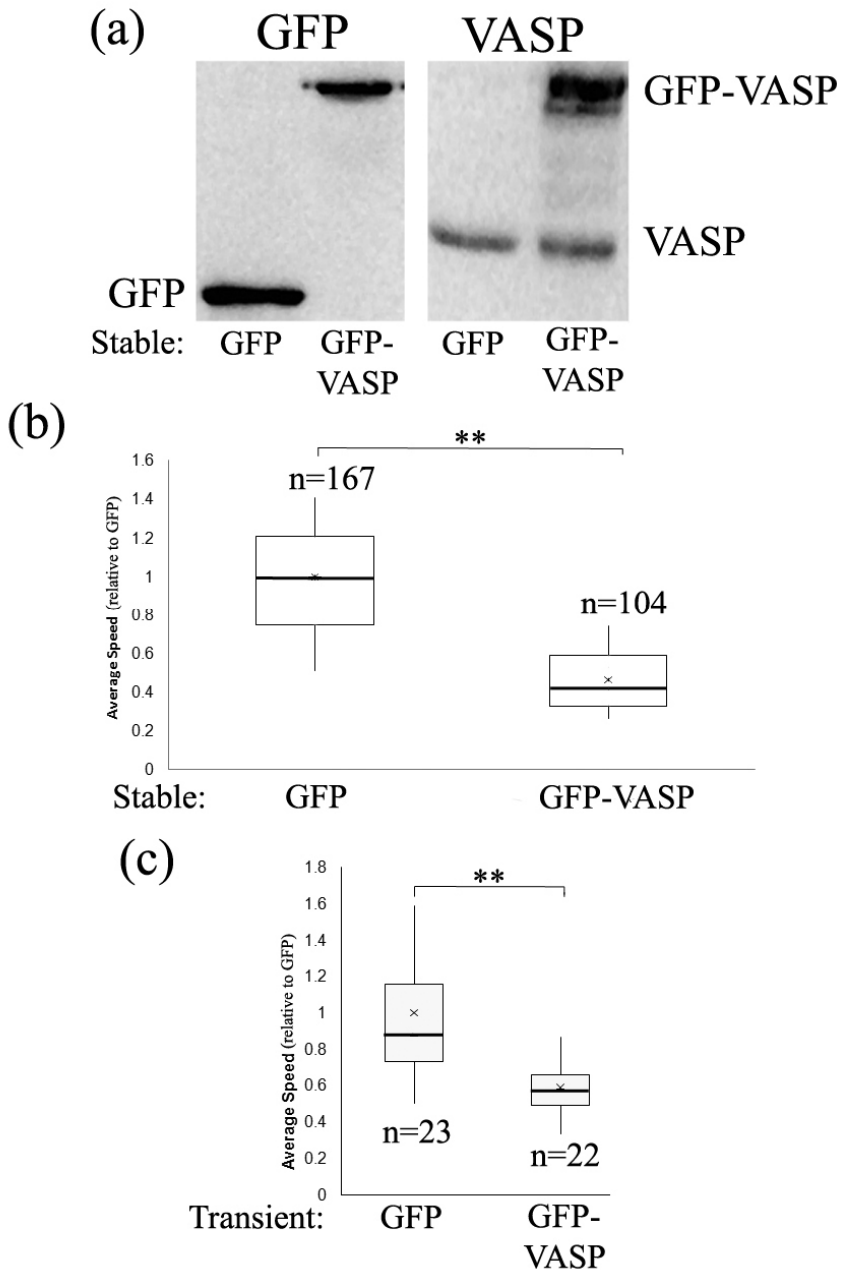

Figure 10. VASP overexpression reduces motility. (a) GFP (left panel) and VASP (right panel) immunoblot of stably transfected GFP and GFP-VASP MDA-231 over-expressers. (b) A box and whisker plot comparing the average speed of stable GFP and GFP-VASP MDA-231 cells (n—number of analyzed cells pooled from 3-4 experiments). All results are normalized to mean stable GFP speed. Double asterisks represent P<.01 (c) A box and whisker plot comparing the average speed of transiently transfected GFP and GFP-VASP MDA-231 cells.

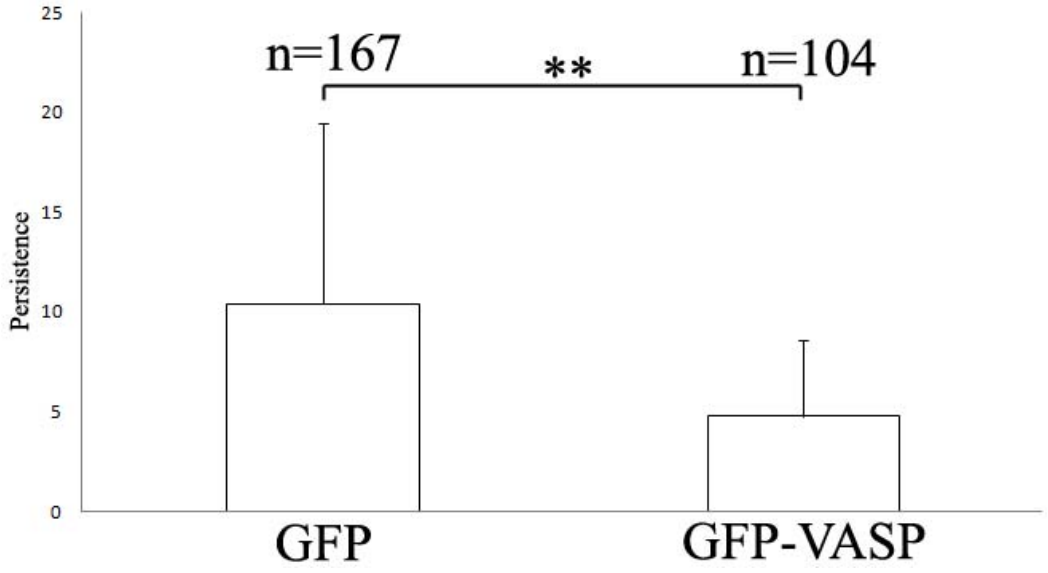

Figure 11. Persistence is reduced in VASP overexpressing cells. (a) Bar graph depicting persistence (per minute) of stable groups (n represents number of cells). Double asterisk signify P<.01.

5.1.3 VASP and Pfn1 interaction is required for negative regulation of cell motility

I next asked whether VASP overexpression induced impaired motility of MDA-231 requires interaction with Pfn1. To address this question, I re-evaluated the motility of GFP and GFP-VASP overexpressers either in wild-type or a polyproline binding deficient mutant Pfn1 background. These two Pfn1 backgrounds were created by silencing endogenous Pfn1 expression and then rescuing with either wild-type or H133S mutant (this mutant of Pfn1 fails to bind polyproline and thus does not interact with VASP) of CFP-Pfn1. Figure 12b shows that when GFP-VASP is overexpressed in H133S-Pfn1 background, it only causes a 20% reduction in the speed compared to 50% reduction seen in wild-type Pfn1 background. In a complementary set of experiments, I transiently transfected MDA-231 with GFP, GFP-VASP or GFP-VASP-P120E/L210E (a mutant form of VASP where the regulatory and loading site have been mutated to significantly reduce VASP's binding to Pfn1) and examined the motility. Figure 12c shows that this mutant form of VASP is less efficient than wild-type VASP (24% vs. 50%) in terms of suppressing random motility of MDA-231 cells. Together these two sets of experimental data clearly suggest that VASP utilizes Pfn1's interaction to regulate cell motility.

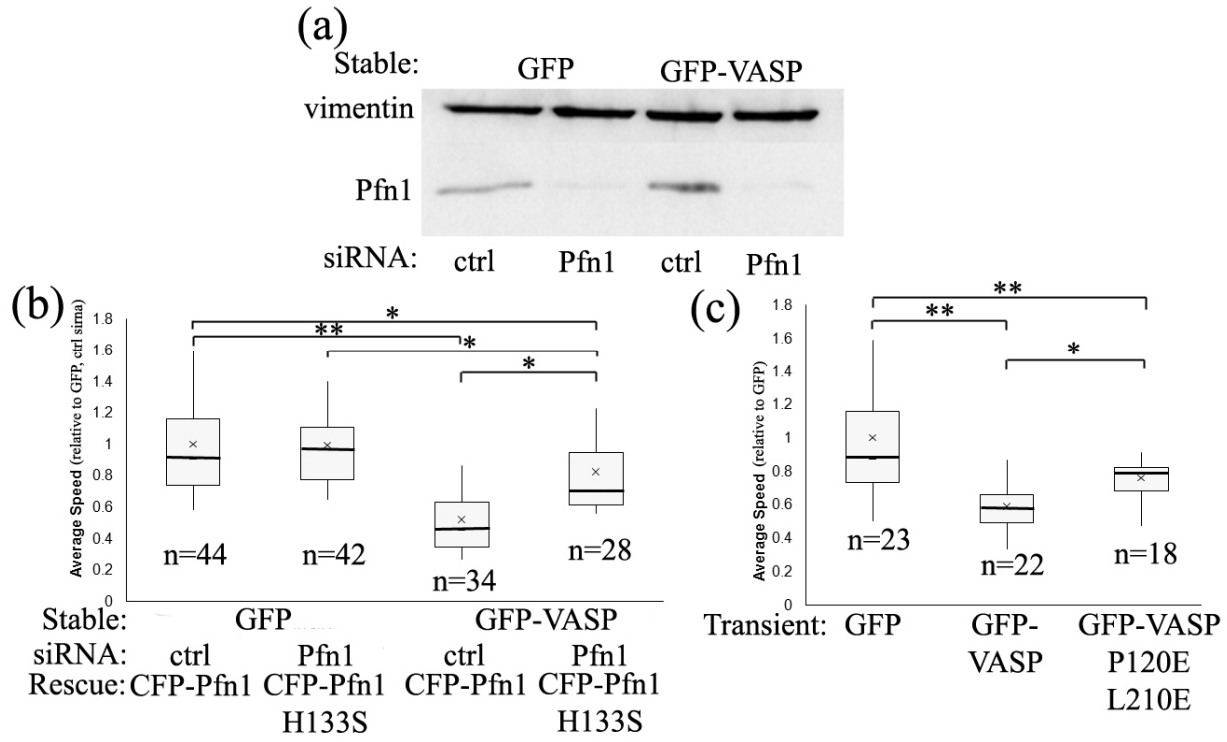

Figure 12. VASP requires interaction with Pfn1 to negatively regulate cell motility. (a) Pfn1 immunoblot of ctrl and Pfn1 siRNA stable MDA-231 cells. Vimentin represents a loading control. (b) Box and whiskers plot of ctrl vs. Pfn1 knockdown in stably expressing GFP or GFP-VASP MDA-231 with either CFP-Pfn1 or CFP-Pfn1-H133S rescued. (n represents number of cells). Asterisk and double asterisk denote P<.05 and P<.01 respectively. (c) Box and whiskers plot of random migration for transiently transfection GFP, GFP-VASP, GFP-VASP P120E/L210E MDA-231 cells.

5.2 DISCUSSION

Ena/VASP proteins have been well characterized thus far as promoters of membrane protrusion through their role as an actin elongator [Rottner et al., 1999]. VASP has also been shown to increase the speed of *Listeria* movement intracellularly through the polyproline domain [Geese et al., 2002]. The polyproline domain of VASP was shown to be required for *Listeria* motility but not for whole cell migration, at least for fibroblasts. Studies on the polyproline domain of VASP however utilize a deletion of the region. Deletion of the polyproline domain not only abrogates binding to Pfn1 but also to SH3- and WW- domain which may cause further confounding data. This study aimed to identify key effects of VASP and Pfn1 interaction on cell migration using complementary mutation on VASP for the first time.

We found that a significant fraction of cells following Mena/VASP knockdown assumed an elongated morphology lacking proper lamellipodia. This is consistent with the role of Ena/VASP in membrane protrusion. With only VASP silenced, there was no noticeable difference of random motility between ctrl and VASP siRNA groups. VASP is only one of three members in the Ena/VASP family however. By silencing VASP, a phenotype may not be induced because of the possibility that the other two members may compensate for the lack of VASP. Silencing Mena and VASP led to a slight reduction of motility. Average speed of migration may be reduced because silencing Mena and VASP removes a majority of F-actin elongators. The phenotype created by Mena/VASP knockdown may also be minor due to an incomplete knockdown of Mena and VASP. In addition, EVL is still present in the cell and may compensate for the lack of Mena and VASP.

Since VASP knockdown alone did not produce a phenotype, I pursued the effect of VASP overexpression. Migration assays were conducted on stable GFP and GFP-VASP

overexpressing MDA-231 cells. Both stable expressing and transiently transfected groups showed a reduced speed in random motility when GFP-VASP was overexpressed. VASP has been implicated as an anti-cappper. Thus, when VASP is overexpressed, the net anti-capping action of VASP is expected to increase. Capping proteins act to prevent unwanted or unproductive F-actin elongation. Unproductive protrusion can lead to counteractive protrusion which leads to less net distance travelled for cells. As an F-actin elongator and capping protein antagonizer, overexpressed VASP would be expected to create longer actin filaments. In addition, overexpression of VASP could increase side binding of VASP to actin filaments. This may prevent binding of Arp2/3 to the sides of filaments and reduce branching of filaments. Long actin filaments tend to buckle more and this causes a protrusion to withdraw. Overall, overexpression of VASP and knockdown of Mena/VASP reduced random motility of MDA-231, thus suggesting that too much or too little Ena/VASP may be detrimental to random motility.

I next investigated the role of VASP:Pfn1 interaction. I performed a silence and rescue of Pfn1 levels with either Pfn1 or Pfn1-H133S. The H133S mutant form of Pfn1 prevents Pfn1 from interacting with PLPs. With the rescue experiment, I show that once again VASP down regulation of random motility is reduced without interaction with Pfn1. The complementary experiment is a novel way to investigate VASP:Pfn1 interaction and does not utilize the deletion of the polyproline region. By only mutating key amino acids of the Pfn1 binding sites on VASP, SH3- and WW-domains are preserved. Mutation of the regulatory site and loading site caused a recovery of motility similar to the effects of Pfn1-H133S rescue. While VASP does not require Pfn1 to function, interaction with Pfn1 enhances the abilities of VASP [Barzik et al., 2005; Hansen et al., 2010]. Through the Pfn1 binding sites of VASP, VASP is able to recruit actin to the growing ends of F-actin through Pfn1. With the H133S mutant or mutant form of VASP,

Pfn1 can no longer bind to VASP, thus reducing its elongation abilities. Pfn1 can still shuttle actin to the leading edge however without interaction with VASP which may explain why motility was not fully recovered.

In essence, this study showed the effects of VASP overexpression or silencing on MDA-231 random motility. I also showed that Pfn1:VASP negatively regulates random migration speed of MDA-231. Future experiments should work to determine actin dynamics along with Pfn1:VASP interaction. Further work should also be performed to determine which polyproline site is the most important for cell migration.

6.0 CONCLUSIONS

The work presented here further clarifies the relationship between VASP and Pfn1 in cell migration. Using acceptor photobleaching FRET, I have shown that Pfn1:VASP interaction occurs near the leading edge of motile MDA-231 cells. This answers the question of spatial interaction between Pfn1 and VASP which biochemical methods in the past could not show. While acceptor photobleaching FRET is useful for determining protein-protein interaction, this technique cannot show dynamics of the interaction. Furthermore, this study showed that VASP indeed plays a role in cell migration (at least in MDA-231). Overexpression of VASP reduces motility most likely through its role as an anti-capper. By overexpressing VASP, less capping protein will be bound to growing ends of F-actin. This prevents capping of unwanted protrusions and leads to counteractive actin polymerization. Finally, using a rescue system and a novel VASP mutation expression, I demonstrated that VASP was not able to reduce motility as well without its binding partner Pfn1 which means that VASP and Pfn1 negatively regulate cell migration. In essence, this study further clarifies the *in vivo* effects of VASP:Pfn1 interaction in motile MDA-231 cells.

6.1 FUTURE DIRECTION

This study showed that VASP and Pfn1 interaction played a negative regulatory role in cell migration. But how VASP:Pfn1 interaction inhibits cell motility remains to be identified. Future studies should be conducted to determine whether abolishing VASP:Pfn1 interaction alters the overall architrecture of actin filaments in the lamellipodia, actin dynamics at the leading edge and distribution of other actin-regulatory proteins (such as capping protein and Arp 2/3).

BIBLIOGRAPHY

Allen P. (2003). Actin filament uncapping localizes to ruffling lamellae and rocketing vesicles. *Nat Cell Biol* **5**: 972-979.

Bachmann C, Fisher L, Walter U, Reinhard, M. (1999). The EVH2 domain of the vasodilator-stimulated phosphoprotein mediates tetramerization, F-actin binding, and actin bundle formation. *J. Biol. Chem.* **274**:23549-57.

Bae YH, **Johnson PA**, **Florek CA**, **Kohn J**, **Moghe PV**. (2006). Minute changes in composition of polymer substrates produce amplified differences in cell adhesion and motility via optimal ligand conditioning. *Acta Biomater* **2**: 473-482.

Bae YH, Ding Z, Zou L, Wells A, Gertler F, Roy P. (2009). Loss of profilin-1 expression enhances breast cancer cell motility by Ena/VASP proteins. *J Cell Physiol* **219**: 354-364.

Ball LJ, Kuhne R, Hoffmann B, Hafner A, Schmieder P. (2000). Dual epitope recognition by the VASP EVH1 domain modulates polyproline ligand specificity and binding affinity. *EMBO J.* **19**:4903-4914.

Barzik M, Kotova TI, Higgs HN, Hazelwood L, Hanein D, Gertler FB, Schafer DA. (2005). Ena/VASP proteins enhance actin polymerization in the presence of barbed end capping proteins. *J Biol Chem* **280**: 28653-28662.

Bear JE, Loureiro JJ, Libova I, Fassler R, Wehland J, Gertler FB. (2000). Negative regulation of fibroblast motility by Ena/VASP proteins. *Cell* **101**: 717-728.

Bear JE, Svitkina TM, Krause M, Schafer DA, Loureiro JJ, Strasser GA, Maly IV, Chaga OY, Cooper JA, Borisy GG, Gertler FB. (2002). Antagonism between Ena/VASP proteins and actin filament capping regulates fibroblast motility. *Cell* **109**: 509-521.

Belot, N., Pochet, R., Heizmann, C. W., Kiss, R. and Decaestecker, C. (2002). Extracellular S100A4 stimulates the migration rate of astrocytic tumor cells by modifying the organization of their actin cytoskeleton. *Biochim Biophys Acta* **1600**: 74-83.

Buss, F., Temm-Grove, C., Henning, S. and Jockusch, B. M. (1992). Distribution of profilin in fibroblasts correlates with the presence of highly dynamic actin filaments. *Cell Motil Cytoskeleton* **22**: 51-61.

Chen P, Murphy-Ullrich J, Wells A. (1996). A role for gelsolin in actuating epidermal growth factor receptor-mediated cell motility. *J Cell Biol* **134**: 689-698.

Chaudhary A *et al.* (1998). Probing the phosphoinositide 4,5-bisphosphate binding site of human profilin I. *Chem Biol* **5**: 273-281.

Clark EA, Golub TR, Lander S, Hynes RO. (2000). Genomic analysis of metastasis reveals an essential role of RhoC. *Nature* **406**: 532-535.

Dickinson R and Tranquillo R. (2004). Optimal estimation of cell movement indices from the statistical analysis of cell tracking data. *AIChE* **39**: 1995-2010.

Ding Z, Lambrechts A, Parepally M, Roy P. (2006). Silencing profilin-1 inhibits endothelial cell proliferation, migration and cord morphogenesis. *J Cell Sci* **119**: 4127-4137.

Ding Z, Gau D, Deasy B, Wells, A, Roy P. (2009). Both actin and polyproline interactions of Profilin-1 are required for migration, invasion and capillary morphogenesis of vascular endothelial cells. *Exp Cell Res* **315**: 2963-2973.

Fedorov AA *et al.* (1994). X-ray structures of isoforms of the actin-binding protein profilin that differ in their affinity for phosphatidylinositol phosphates. *Proc Natl Acad Sci U S A* **91**: 8636-8640.

Ferron F, Rebowski G, Lee S, Dominguez R. (2007). Structural basis for the recruitment of profilin-actin complexes during filament elongation by Ena/VASP. *EMBO*. **26**: 4597-4606.

Gau, D, Ding Z, Baty C, Roy P. (2011) Fluorescence Resonance Energy Transfer (FRET)-based detection of profilin-VASP interaction. *Cell. Mol. Bioeng.* **4**: 1-8.

Geese, M. *et al.* (2002) Contribution of Ena/VASP proteins to intracellular motility of listeria requires phosphorylation and proline-rich core but not F-actin binding or multimerization. *Mol. Biol. Cell* **13**: 2383-96.

Gertler FB, Niebuhr K, Reinhard M, Wehland J, Soriano P. (1996). Mena, a relative of VASP and *Drosophila*Enabled, is implicated in the control of microfilament dynamics. *Cell*. **87**:227-39.

Goldschmidt-Clermont PJ, Machesky LM, Baldassare JJ, Pollard TD. (1990). The actin-binding protein profilin binds to PIP2 and inhibits its hydrolysis by phospholipase C. *Science* **247**: 1575-1578.

Goldschmidt-Clermont PJ *et al.* (1991). Regulation of phospholipase C-gamma 1 by profilin and tyrosine phosphorylation. *Science* **251**: 1231-1233.

Gronborg, M., Kristiansen, T. Z., Iwahori, A., Chang, R., Reddy, R., Sato, N., Molina, H.,Jensen, O. N., Hruban, R. H., Goggins, M. G. et al. (2006). Biomarker discovery from pancreatic cancer secretome using a differential proteomic approach. *Mol Cell Proteomics* **5**:157-71.

Hansen, S.D. and Mullins, R.D. (2010) VASP is a processive actin polymerase that requires monomeric actin for barbed end association. *J. Cell Biol.* **191**: 571-84.

Haugwitz M, Noegel AA, Karakesisoglou J, Schleicher M. (1994). Dictyostelium amoebae that lack G-actin-sequestering profilins show defects in F-actin content, cytokinesis, and development. *Cell* **79**: 303-314.

Holt MR, Koffer A. (2001). Cell motility: Proline-rich proteins promote protrusions. *Trends Cell Biol* **11**: 38-46.

Janmey P. (1994). Phosphoinositides and calcium as regulators of cellular actin assembly and disassembly. *Annu Rev Physiol* **56**: 169-191.

Janke, J., Schluter, K., Jandrig, B., Theile, M., Kolble, K., Arnold, W., Grinstein, E., Schwartz, A., Estevez-Schwarz, L., Schlag, P. M. et al. (2000). Suppression of Tumorigenicity in breast cancer cells by the microfilament protein profilin 1. *J Exp Med* **191**: 1675-86.

Jockusch, B. M., K. Murk, and M. Rothkegel. (2007). The profile of profilins. Rev. Physiol. Biochem. Pharmacol. **159**:131– 149.

Kang F, Laine RO, Bubb MR, Southwick FS, Purich DL. (1997). Profilin interacts with the Gly-Pro-Pro-Pro-Pro-Pro sequences of vasodilator-stimulated phosphoprotein (VASP): implications for actin-based Listeria motility. *Biochemistry* **36**: 8384-8392.

Kang F, Purich DL, Southwick FS. (1999). Profilin promotes barbed-end actin filament assembly without lowering the critical concentration. *J Cell Biol* **274**: 36963-36972.

Karlsson L, Nystrom LE, Sundkvist I, Markey F, Lindberg U. (1977). Actin polymerizability is influenced by profilin, a low molecular weight protein in non-muscle cells. *J Mol Biol* **115**: 465-483.

Karpova, T. S., C. T. Baumann, L. He, X. Wu, A. Grammer, P. Lipsky, G. L. Hager, and J. G. McNally. (2003). Fluorescence resonance energy transfer from cyan to yellow fluorescent protein detected by acceptor photobleaching using confocal microscopy and a single laser. J. Microsc. **209**(Pt 1):56–70.

Krause M, Leslie JD, Stewart M, Lafuente EM, Valderrama F, Jagannathan R, Strasser GA, Rubinson DA, Liu H,Way M, Yaffe MB, Boussiotis VA, Gertler FB. (2004). Lamellipodin, an Ena/VASP ligand, is implicated in the regulation of lamellipodial dynamics. *Dev Cell* **7**: 571-583.

Krause M, Dent E, Bear J, Loureiro J, Gertler FB. (2003). Ena/VASP Proteins: Regulators of the Actin Cytoskeleton and Cell Migration. *Annu. Rev. Cell Dev. Biol* **19**: 541-564.

Lacayo CI, Pincus Z, VanDuijn MM, Wilson CA, Fletcher DA, Gertler FB, Mogilner A, Theriot JA. (2007). Emergence of large-scale cell morphology and movement from local actin filament growth dynamics. *PLoS Biol* **5**: e233.

Lassing I, Lindberg U. (1985). Specific interaction between PI(4,5)P2 and profilactin. *Nature* **314**: 472-474.

Lassing I, Lindberg U. (1998). Specificity of the interaction between phosph**a**tidylinositol 4,5-bisphosphate and the profilin:actin complex. *J Cell Biochem* **37**: 255-267.

Le Clainche, C. and Carlier, M.F. (2008) Regulation of actin assembly associated with protrusion and adhesion in cell migration. *Physiol. Rev.* **88**: 489-513.

Loisel, T.P. *et al.* (1999) Reconstitution of actin-based motility of Listeria and Shigella using pure proteins. *Nature* **401**: 613-6.

Lorenz, M. *et al*. (2004) Imaging sites of N-WASP activity in lamellipodia and invadopodia of carcinoma cells. *Curr. Biol.* **14**: 697-703.

Lu J, Pollard TD. (2001). Profilin binding to poly-L-proline and actin monomers along with ability to catalyze actin nucleotide exchange is required for viability of fission yeast. *Mol Biol Cell* **12**: 1161-1175.

Mahoney NM *et al.* (1999). Profilin binds proline-rich ligands in two distinct amide backbone orientations. *Nat Struct Biol* **6**: 666-671.

Mayboroda, O., Schluter, K. and Jockusch, B. M. (1997). Differential colocalization of profilin with microfilaments in PtK2 cells. *Cell Motil Cytoskeleton* **37**: 166-77.

Metzler WJ *et al.* (1994). Identification of the poly-L-proline-binding site on human profilin. *J Biol Chem* **269**: 4620-4625.

Mimuro, H. *et al.* (2000) Profilin is required for sustained efficient intra- and intercellular spreading of shigella flexneri. *J. Biol. Chem.* **275**: 28893-901.

Neely, M. D. and Macaluso, E. (1997). Motile areas of leech neurites are rich in microfilaments and two actin-binding proteins: gelsolin and profilin. *Proc Biol Sci* **264**: 1701-6.

Panetti TS, **Hannah DF**, **Avraamides C**, **Gaughan JP**, **Marcinkiewicz C**, **Huttenlocher A**, **Mosher DF**. (2004). Extracellular matrix molecules regulate endothelial cell migration stimulated by lysophosphatidic acid. *J Thromb Haemost* **2**: 1645-1656.

Pantaloni D, Carlier MF. (1993). How profilin promotes actin filament assembly in the presence of thymosin beta-4. *Cell* **75**: 1007-1014.

Pollard TD, Borisy GG. (2003). Cellular motility driven by assembly and disassembly of actin filaments. *Cell* **112**: 453-465

Reinhard, M., K. Giehl, K. Abel, C. Haffner, T. Jarchau, V. Hoppe, B. M. Jockusch, and U. Walter. (1995) The proline-rich focal adhesion and microfilament protein VASP is a ligand for profilins. EMBO J. **14**(8):1583–1589.

Ridley AJ, Schwartz MA, Burridge K, Firtel RA, Ginsberg MH, Borisy G, Parsons JT, Horwitz AR. (2003). Cell migration: integrating signals from front to back. *Science* **302**: 1704-1709.

Romero, S. *et al.* (2004) Formin is a processive motor that requires profilin to accelerate actin assembly and associated ATP hydrolysis. *Cell* **119**: 419-29.

Rottman JB. (1999). Key role of chemokines and chemokine receptors in inflammation, immunity, neoplasia, and infectious disease. *Vet Pathol* **36**: 357-367.

Rottner, K., B. Behrendt, J. V. Small, and J. Wehland. (1999). VASP dynamics during lamellipodia protrusion. Nat. Cell Biol. **1**(5):321–322.

Roy, P., Z. Rajfur, P. Pomorski, and K. Jacobson. (2002). Microscope-based techniques to study cell adhesion and migration. Nat. Cell Biol. **4**(4):E91–E96.

Roy P, Jacobson K. (2004). Overexpression of profilin reduces the migration of invasive breast cancer cells. *Cell Motil Cytoskeleton* **57**: 84-95.

Schluter K, Jockusch BM, Rothkegel M. (1997). Profilin as regulators of actin dynamics. *Biochim Biophys Acta* **1359**: 97-109.

Sheetz MP, Felsenfeld D, Galbraith CG, and Choquet D. (1999). Cell migration as a five-step cycle. *Biochem Soc Symp* **65**: 233-243.

Skare P, Karlsson R. (2002). Evidence for two interaction regions for phosphatidylinositol (4,5)-bisphosphate on mammalian profilin I. *FEBS Lett* **522**: 119-124.

Stradal, T.E. and Scita, G. (2006) Protein complexes regulating Arp2/3-mediated actin assembly. *Curr. Opin. Cell Biol.* **18**: 4-10.

Suetsugu, S. *et al.* (1998) The essential role of profilin in the assembly of actin for microspike formation. *EMBO J.* **17**: 6516-26.

Tomasevic, N. *et al.* (2007) Differential regulation of WASP and N-WASP by Cdc42, Rac1, Nck, PI(4,5)P2. *Biochemistry* **46**: 3494-502.

van Rheenen J, Song X, van Roosmalen W, Cammer M, Chen X, Desmarais V, Yip SC, Backer JM, Eddy RJ, Condeelis JS. (2007). EGF-induced PIP2 hydrolysis releases and 86 activates cofilin locally in carcinoma cells. *J Cell Biol* **179**: 1247-1259.

Velarde, N., Gunsalus, K. C. and Piano, F. (2007). Diverse roles of actin in C. elegans early embryogenesis. *BMC Dev Biol* **7**: 142.

Verheyen EM, Cooley L. (1994). Profilin mutations disrupt multiple actin-dependent processes during drosophila development. *Development* **120**: 717-728.

Walders-Harbeck B, Khaitlina SY, Hinssen H, Jockusch BM, Illenberger S. (2002). The vasodilator-stimulated phosphoprotein promotes actin polymerization through direct binding to monomeric actin. *FEBS Lett.* **529**:275-80.

Wang FL,Wang Y, Wong WK, Liu Y, Addivinola J, Liang P, Chen LB, Kantoff PW, Pardee AB. (1996). Two differentially expressed genes in normal human prostate tissue and in carcinoma. *Cancer Res* **56**: 3634-3637.

Weisner, S. *et al.* (2003) A biomimetic motility assay provides insight into the mechanism of actin-based motility. *J. Cell Biol.* **160**: 387-98.

Witke, W. (2004). The role of profilin complexes in cell motility and other cellular processes. Trends Cell Biol. **14**(8):461–469.

Wittenmayer, N., M. Rothkegel, B. M. Jockusch, and K. Schluter. (2000). Functional characterization of green fluorescent protein-profilin fusion proteins. Eur. J. Biochem. **267**(16):5247–5246.

Wittenmayer, N., Jandrig, B., Rothkegel, M., Schluter, K., Arnold, W., Haensch, W., Scherneck, S. and Jockusch, B. M. (2004). Tumor suppressor activity of profilin requires a functional actin binding site. *Mol Biol Cell* **15**: 1600-8.

Zou L, Jaramillo M, Whaley D, Wells A, Panchapakesa V, Das T, Roy P. (2007). Profilin-1 is a negative regulator of mammary carcinoma aggressiveness. *Br J Cancer* **97**: 1361-1371.

Zou L, Hazan R, Roy P. (2009). Profilin-1 overexpression restores adherence junctions in MDA-MB-231 breast cancer cells in R-cadherin-dependent manner. *Cell Motil Cytoskeleton*. **66**(12):1048-1056.